

# Spontaneous Pattern Formation Induced by Ion Bombardment of Binary Compounds

R. Mark Bradley

*Department of Physics, Colorado State University, Fort Collins, Colorado 80523, USA*

Patrick D. Shipman

*Department of Mathematics, Colorado State University, Fort Collins, Colorado 80523, USA*

(Received 22 June 2010; revised manuscript received 12 August 2010; published 1 October 2010)

A theory is developed that explains the genesis of the strikingly regular hexagonal arrays of nanoscale mounds that can form when a flat surface of a binary compound is subjected to normal-incidence ion bombardment. We find that the species with the higher sputter yield is concentrated at the peaks of the nanodots and that hysteretic switching between the flat and the hexagonally ordered state can occur as the sample temperature is varied. Surface ripples are predicted to emerge for a certain range of the parameters.

DOI: [10.1103/PhysRevLett.105.145501](https://doi.org/10.1103/PhysRevLett.105.145501)

PACS numbers: 81.16.Rf, 05.45.-a, 68.35.Ct, 79.20.Rf

Bombarding a solid surface with a broad ion beam produces a remarkable variety of self-assembled nanoscale patterns [1]. The spontaneous emergence of these patterns is not just fascinating in its own right, since ion bombardment may prove to be an important tool in the fabrication of cutting-edge nanostructures.

The first type of pattern formation to be discovered was the periodic height modulations or “ripples” that often develop when the nominally flat surface of a solid is subjected to oblique-incidence ion bombardment [2]. According to the widely accepted Bradley-Harper (BH) theory [3], ripples are a result of a surface instability caused by the curvature dependence of the sputter yield.

In the BH theory, a solid surface subject to normal-incidence ion bombardment (NIIB) is also unstable. Since the growth rate of the unstable Fourier modes is independent of the direction of the wave vector, it was expected that NIIB would produce a rough, unstructured surface. It therefore came as a considerable surprise when experiments by Facsko *et al.* revealed that NIIB of the binary compound GaSb can result in the formation of nanoscale mounds or “nanodots” arranged in a hexagonal array of astonishing regularity [4]. Well-ordered hexagonal nanodot arrays can also be produced by oblique-incidence ion bombardment of InP if the sample is rotated while it is bombarded [5]. These observations are not just of academic interest: Ion bombardment provides a fast and reproducible means of producing a nearly regular array of quantum dots on a semiconductor surface in a single process step.

In the experiments of Facsko *et al.*, the nanodot size distribution was sharply peaked and the dot arrays had short-range hexagonal order (SRHO) that extended over six or more lattice spacings. These observations strongly suggest that there is a narrow band of unstable wavelengths, according to the modern theory of pattern formation [6]. By contrast, all ripple wavelengths that exceed a critical value are unstable in the linear BH theory and in

theories that add nonlinear terms to the BH equation of motion [7,8].

In this Letter, we advance a theory for the pattern formation that occurs when the initially flat surface of a binary compound is subjected to NIIB. We demonstrate analytically that there is a narrow band of unstable wavelengths and that nanodot arrays with SRHO emerge spontaneously for a certain range of the parameters. Since the hexagonal ordering in the surface height is mirrored in the variations of composition at the surface, NIIB could be used as a tool to simultaneously achieve nanoscale patterning of the surface topography and composition. We also find that hysteretic switching between the flat and hexagonally ordered states can occur as the sample temperature is varied. Finally, our theory makes the exciting prediction that *normal-incidence* bombardment will produce surface ripples for a certain range of the parameters.

When an ion beam impinges on a binary compound, generally one of the components is preferentially sputtered, yielding a surface layer of altered stoichiometry. During the formation of hexagonal arrays of nanodots by NIIB of GaSb, for example, a Ga excess of 30 at. % developed at the surface [9]. The coupling between this altered surface layer and the topography is crucial to the formation of hexagonal arrays of nanodots in our theory. The pioneering work on this coupling is due to Shenoy, Chan, and Chason [10]. We will extend the theory of Shenoy, Chan, and Chason to include the key physical effect that can lead to a narrow band of unstable wavelengths—momentum transfer from the incident ions to atoms at the surface produces surface atomic currents [11]. In addition, nonlinear terms must be added to the linear theory of Shenoy, Chan, and Chason if hexagonal ordering is to occur.

Two theories for the formation of hexagonal arrays of mounds on *elemental* materials have previously been introduced. In the theory of Facsko *et al.*, a linear, highly non-local term is added to the usual Kuramoto-Sivashinsky

equation, yielding the so-called damped Kuramoto-Sivashinsky equation [12]. For appropriate values of the damping parameter, this term does lead to a narrow band of unstable wavelengths and to SRHO. However, there does not seem to be any plausible physical origin for such a term. It has been suggested that the damping term could model redeposition of sputtered material [12], but careful analysis reveals that redeposition leads to the addition of a *nonlinear* term to the equation of motion [13]. Therefore, redeposition cannot produce a narrow band of unstable wavelengths.

In the theory of Castro *et al.*, a mobile surface layer modifies the dynamics, leading to the addition of a second nonlinear term to the Kuramoto-Sivashinsky equation [8]. This theory successfully accounts for the coarsening of the nanodot arrays that is sometimes observed in experiments [4,14,15]. At first, it seemed that the Castro *et al.* nonlinearity might also produce strong SRHO [8], but more recent numerical work shows that the hexagonal order (if present at all) is weak and has very short range [15,16].

Consider a binary solid consisting of atoms of two species, *A* and *B*. Initially, the solid occupies the region with  $z \leq 0$ , and the concentration of *A* atoms,  $c_b$ , is uniform throughout the solid. The solid is now subjected to normal-incidence ion bombardment.

Assume that species *B* is preferentially sputtered. As time passes, an altered surface layer develops in which the concentration of *A* atoms is greater than the bulk value  $c_b$ . For simplicity, we take this surface layer to have thickness  $\Delta$  and uniform concentration  $c_s$ . A steady state is eventually reached in which  $c_s$  has a constant value  $c_{s,0} > c_b$  and in which the surface is eroded at a constant rate, i.e., the surface height  $h = h_0 - v_0 t$ , where  $h_0$  and  $v_0 > 0$  are constants.

Suppose that the planar surface is now perturbed. The surface height  $h = h_0 - v_0 t + u$  and surface concentration  $c_s = c_{s,0} + \phi$  are now functions of  $\mathbf{r} \equiv x\hat{x} + y\hat{y}$  and  $t$ . We assume that subsurface concentration variations have a negligible effect on the collision cascades, following Ref. [10]. Provided that  $u$  is a slowly varying function of  $\mathbf{r}$ , the power deposited by the bombarding ions per unit surface area is then  $P = P_0 + \alpha \nabla^2 u + \beta (\nabla u)^2$ , where  $\nabla \equiv \hat{x}\partial_x + \hat{y}\partial_y$ . The constants  $P_0 > 0$ ,  $\alpha > 0$ , and  $\beta$  have been computed by using the Sigmund theory of sputtering [17] and depend on the ion range and the longitudinal and transverse straggling lengths [3,7,18].

In the Sigmund theory [17], the flux sputtered from the surface of an elemental material is taken to be proportional to  $P$ . For a binary solid, therefore, it is natural to assume that the sputtered fluxes of species *A* and *B* ( $F_A$  and  $F_B$ , respectively) are both proportional to  $P$ : We set  $F_i = \Lambda_i P$  for  $i = A, B$ , where  $\Lambda_A$  and  $\Lambda_B$  depend on  $c_s$ .

Atomic currents on the surface also affect its dynamics. We take the sample temperature  $T$  to be high enough that surface diffusion is thermally activated. For  $i = A, B$ , the surface current of species *i* is then

$$\mathbf{J}_i = -D_i n_s \nabla c_i + \beta_T D_i c_i n_s \Omega \gamma_s \nabla \nabla^2 h - \mu_i \nabla h, \quad (1)$$

where  $D_i$  is the surface diffusivity of species *i* and has an Arrhenius form;  $n_s$  is the total areal density of mobile surface atoms;  $c_A = c_s$  and  $c_B = 1 - c_s$ ;  $\Omega$  is the atomic volume;  $\gamma_s$  is the surface tension; and  $\beta_T \equiv 1/(k_B T)$ . In the first and second terms on the right-hand side of Eq. (1), the areal density of mobile surface atoms of species *i* has been taken to be  $c_i n_s$ . These terms describe surface diffusion's tendency to make the surface concentration of species *i* uniform and to flatten the surface to reduce its energy. Momentum transfer from the incident ions to atoms of species *i* at the surface gives rise to the final term on the right-hand side of Eq. (1); the positive constant  $\mu_i$  characterizes the strength of this smoothing effect [11]. As we shall see, this term plays a crucial role in the pattern formation.

Mass conservation yields

$$\partial_t h = -\Omega(F_A + F_B + \nabla \cdot \mathbf{J}_A + \nabla \cdot \mathbf{J}_B). \quad (2)$$

In addition, because *A* atoms are removed from the solid only by sputtering,

$$l^{-2} \partial_t c_s = (c_b - 1)(F_A + \nabla \cdot \mathbf{J}_A) + c_b(F_B + \nabla \cdot \mathbf{J}_B), \quad (3)$$

where  $l \equiv (\Omega/\Delta)^{1/2}$ . Retaining only terms of first order in  $u$  and  $\phi$  gives an equation of motion of the form

$$\partial_t \boldsymbol{\rho} = \mathbf{M}_1 \phi + \mathbf{M}_2 \nabla^2 \phi + \mathbf{M}_3 \nabla^2 u + \mathbf{M}_4 \nabla^2 \nabla^2 u, \quad (4)$$

where  $\boldsymbol{\rho} \equiv (u, \phi)^T$  and  $\mathbf{M}_i = (M_{i,1}, M_{i,2})^T$ .

A total of eight parameters appear in Eq. (4), and so some simplification of this equation is desirable. Both analytical work and numerical integrations show that the terms proportional to  $M_{2,1}$  and  $M_{4,2}$  have little effect on the pattern formation [13]. Accordingly, we will assume that  $D_A = D_B \equiv D_0$  (so that  $M_{2,1} = 0$ ) and set  $M_{4,2}$  to zero. Only the coupling terms of lowest order then remain, and the nonzero coefficients are given by  $M_{1,1} = -\Omega(\Lambda'_{A,0} + \Lambda'_{B,0})P_0$ ,  $M_{3,1} = \Omega[(\mu_A + \mu_B) - \alpha(\Lambda_{A,0} + \Lambda_{B,0})]$ ,  $M_{4,1} = -D_0 n_s \Omega^2 \gamma_s \beta_T$ ,  $M_{1,2} = [(c_b - 1)\Lambda'_{A,0} + c_b \Lambda'_{B,0}]P_0 l^2$ ,  $M_{2,2} = D_0 n_s l^2$ , and  $M_{3,2} = [(1 - c_b)\mu_A - c_b \mu_B]l^2$ , where  $\Lambda_{i,0} \equiv \Lambda_i(c_{s,0})$  and  $\Lambda'_{i,0} \equiv \Lambda'_i(c_{s,0})$  for  $i = A, B$ . We will restrict our attention to the case  $M_{3,1} < 0$ , so that the surface would be unstable if  $M_{1,1}$  were zero, i.e., if the sputter yields of the two species were equal.

Introducing the dimensionless position  $\tilde{\mathbf{r}} = \sqrt{M_{3,1}/M_{4,1}} \mathbf{r}$ , time  $\tilde{t} = M_{3,1}^2 t / |M_{4,1}|$ , and surface displacement  $\tilde{u} = M_{3,1}^2 u / (|M_{4,1}| M_{1,1})$  and dropping the tildes, we obtain

$$\partial_t u + \nabla^2 \nabla^2 u + \nabla^2 u - \phi = N_1 (\nabla u, \phi) \quad (5)$$

and

$$\partial_t \phi + a\phi - b\nabla^2 u - c\nabla^2 \phi = N_2(\nabla u, \phi), \quad (6)$$

where  $a \equiv M_{1,2}M_{4,1}/M_{3,1}^2$  and  $c \equiv M_{2,2}/|M_{3,1}|$  are positive, but  $b \equiv M_{1,1}M_{3,2}M_{4,1}/M_{3,1}^3$  need only be real.  $N_1$  and  $N_2$  are nonlinear terms that we will add below.

The linearized equations of motion (5) and (6) with  $N_1 = N_2 = 0$  have solutions of the form  $\boldsymbol{\rho} = (u_*, \phi_*)^T \times \exp(i\mathbf{k} \cdot \mathbf{r} + \sigma t)$ , where  $u_*$  and  $\phi_*$  are constants and  $\mathbf{k} \equiv k_x \hat{x} + k_y \hat{y}$ .  $\text{Re}\sigma$  gives the rate with which the amplitude of the mode grows (for  $\text{Re}\sigma > 0$ ) or attenuates (for  $\text{Re}\sigma < 0$ ). For each wave vector  $\mathbf{k}$ , there are two possible values of  $\sigma$ , which we denote by  $\sigma_+$  and  $\sigma_-$ . We adopt the convention that  $\text{Re}\sigma_+ \geq \text{Re}\sigma_-$ .

We will restrict our attention to the region of the parameter space in which  $c > a$  and  $4a > (1 - c)^2$  if  $c < 1$ , since hexagonal ordering occurs in this region. Detailed analysis reveals that the uniform steady state  $\boldsymbol{\rho} = \boldsymbol{\rho}_0 \equiv 0$  is stable for  $b > b_T \equiv (a + c)^2/(4c)$  and is unstable for  $b < b_T$ . In particular, for given values of the parameters  $a$  and  $c$ ,  $\text{Re}\sigma_+(k) < 0$  for all  $k$  if  $b > b_T$ . For  $b = b_T$ ,  $\sigma_+$  vanishes for  $k = k_T \equiv \sqrt{(c - a)/(2c)}$  and  $\text{Re}\sigma_+(k)$  is negative for  $k \neq k_T$ . Finally, for  $b$  just below  $b_T$ , a narrow band of wave numbers develops around  $k_T$  in which  $\text{Re}\sigma_+(k) > 0$  and  $\text{Im}\sigma_+(k) = 0$ . A Turing instability therefore occurs at the point  $b = b_T$  [6].

Once the linear instability has set in, the deviations from the steady state grow progressively larger, and nonlinear terms must be included in the equations of motion. There are two key sources of nonlinearity: The term  $\beta(\nabla u)^2$  appears in  $P$ , and the  $\Lambda_i$ 's are nonlinear functions of  $c_s$  [19,20]. Adding the resulting dominant nonlinear terms to the original linearized equations of motion [13], we obtain  $N_1 = \lambda(\nabla u)^2$  and  $N_2 = \nu\phi^2 + \eta\phi^3$ . Here the term  $N_1$  comes from the slope dependence of the sputter yields,  $\nu$  and  $\eta$  depend on derivatives of the  $\Lambda_i$ 's evaluated at  $c_s = c_{s,0}$ , and we assume that  $\eta > 0$  so that the amplitude of the surface disturbance saturates at long times, as observed experimentally. We omit any additional nonlinear terms for simplicity and because other terms of this kind merely modify the coefficients  $\tau$  and  $\gamma$  defined below.

We now carry out a weakly nonlinear analysis of Eqs. (5) and (6). The bifurcation parameter  $b$  is taken to be slightly below the critical value  $b_T$ : We set  $b = b_T - \epsilon b_1$ , where  $\epsilon > 0$  is small and  $b_1$  is of order 1 and is positive. There is then a narrow band of wave numbers centered on  $k = k_T$  with  $\text{Re}\sigma_+(k) > 0$ . The analysis yields ordinary differential equations for the time evolution of the amplitudes of these unstable modes [6] and proceeds as follows: We set  $\boldsymbol{\rho} = \boldsymbol{\rho}_0 + \epsilon\boldsymbol{\rho}_1 + \epsilon^2\boldsymbol{\rho}_2 + \dots$ . We also introduce the multiple time scales  $t_n \equiv \epsilon^n t$  with  $n = 0, 1, 2, \dots$  and treat these as independent variables, so that  $\partial_t = \partial_{t_0} + \epsilon\partial_{t_1} + \epsilon^2\partial_{t_2} + \dots$ . Finally, we equate the coefficients of like powers of  $\epsilon$  in Eqs. (5) and (6).

We obtain approximate solutions of the form

$$\boldsymbol{\rho} = \frac{1}{4c^2} \sum_{j=1}^3 \left( \frac{4c^2}{a^2 - c^2} \right) \left( A_j e^{i\mathbf{k}_j \cdot \mathbf{r}} + \text{c.c.} \right) + \begin{pmatrix} B \\ 0 \end{pmatrix},$$

where  $\mathbf{k}_1 + \mathbf{k}_2 + \mathbf{k}_3 = 0$  and  $|\mathbf{k}_j| = k_T$  for  $j = 1, 2, 3$ . Solvability conditions for the correction  $\boldsymbol{\rho}_2$  yield equations for the complex amplitudes  $A_j$  and the real amplitude  $B$ . We find that

$$\dot{A}_j = \sigma A_j + \tau A_p^* A_q^* - \gamma A_j (|A_j|^2 + 2|A_p|^2 + 2|A_q|^2), \quad (7)$$

where  $j, p, q \in \{1, 2, 3\}$  are in cyclic order. Here  $\sigma = (b_T - b)f_1$ ,  $\tau = \nu f_2 + \lambda f_3$ , and  $\gamma = \eta f_4$ , where  $f_1, \dots, f_4$  are positive functions of  $a$  and  $c$  too complex to be given here. We also obtain an equation (omitted for the sake of brevity) that gives  $\dot{B}$  as a function of the  $A_j$ 's and that describes how the net sputter yield evolves in time.

The dimensionless ratio  $\xi \equiv \sigma\gamma/\tau^2$  is a measure of the relative strengths of the linear instability and the quadratic and cubic nonlinearities. The amplitude equations (7) admit stationary solutions of three different types [6] that are stable for some range of  $\xi$ . (i) Homogeneous state:  $A_1 = A_2 = A_3 = 0$ .—This solution is the undisturbed steady state  $u = \phi = 0$  and is stable for  $\xi < 0$ . (ii) Roll pattern:  $A_1 = \pm(\tau/\gamma)\xi^{1/2}$ ,  $A_2 = A_3 = 0$ , or cyclic permutations.—These solutions are surface ripples (or ‘‘rolls’’) with wavelength  $2\pi/k_T$  and are stable for  $\xi > 1$ . (iii) Hexagonal pattern:  $A_1 = A_2 = A_3 = \tau(1 + \sqrt{1 + 20\xi})/(10\gamma)$ .—This solution is stable for  $-1/20 < \xi < 4$ . If the sign of the amplitude is positive (negative), the surface  $u$  consists of peaks (dimples) arranged in a hexagonal array. This hexagonal order arises because the quadratic nonlinearities cause the rolls with wave vectors  $\mathbf{k}_1, \mathbf{k}_2$ , and  $\mathbf{k}_3$  to resonate: For example, if  $A_1 = 0$  but  $A_2$  and  $A_3$  are small and positive,  $|A_1|$  will begin to grow.

Numerical integrations of Eqs. (5) and (6) were performed on a  $128 \times 128$  spatial grid with periodic boundary conditions using a Fourier spectral method. Two simulations with a low amplitude white noise initial condition are shown in Fig. 1. The same parameter values were used in both simulations, except that  $\nu = 1$  and  $\xi = 1.16$  for the simulation shown in Figs. 1(a) and 1(b), whereas  $\nu = 0.1$  and  $\xi = 116$  in Figs. 1(c) and 1(d). Clearly, as a quantitative study bears out [13], there is an increase in the correlation length and the amplitude of the peaks in the autocorrelation function as time passes. Consistent with our analysis, the steady-state planform is a regular hexagonal pattern for  $\xi = 1.16$  and rolls for  $\xi = 116$ . The hexagonal order in Fig. 1(b) is strong and of considerable range, as in experiments on GaSb [4]. Finally, the maxima in  $\phi$  occur at the minima of  $u$ , in accord with our approximate solution.

The fundamental finding of this Letter is that the coupling of the surface height to the surface composition can

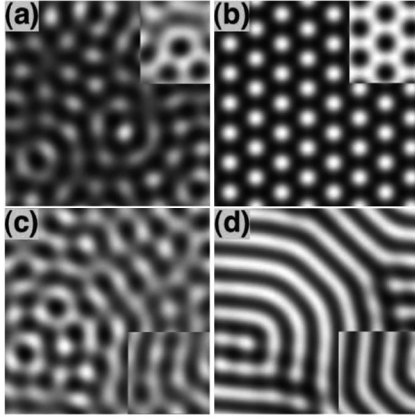


FIG. 1. Gray scale plots of  $u$  in the region  $-40 \leq x, y \leq 40$  with parameter values  $a = 0.25$ ,  $c = 1$  (so that  $b_T \cong 0.391$ ),  $b = 0.365$ ,  $\eta = 10$ , and  $\lambda = 0$ . In (a) and (b),  $\nu = 1$ , whereas  $\nu = 0.1$  in (c) and (d). The times are (a)  $t = 400$ , (b)  $t = 3000$ , (c)  $t = 250$ , and (d)  $t = 1000$ . The shading is dark (light) where  $u$  is large (small). Insets: Gray scale plots of  $\phi$  which cover and are in alignment with the plots of  $u$ . The shading is dark (light) where  $\phi$  is large (small).

lead to a narrow band of linearly unstable wavelengths and so to the formation of nanodot arrays with short-range hexagonal ordering. This comes about because for  $b > a$ , a novel smoothing effect suppresses the small- $k$  instability. To order  $k^2$ , the eigenvector associated with the growth rate  $\sigma_+ = (1 - b/a)k^2$  is  $(u_*, \phi_*)^T = (1, -bk^2/a)^T$ . This shows that for  $b > 0$ , the modulations of the concentration and surface height are out of phase in the Fourier mode with wave vector  $\mathbf{k}$ . From a physical standpoint, ion-induced surface flow produces a net flow of species  $A$  from the surface peaks to the adjacent depressions for  $b > 0$ , i.e., for sufficiently large  $\mu_A/\mu_B$ . Because species  $A$  has a lower sputter yield than species  $B$ , as an excess of  $A$  accumulates in the depressions, there is a tendency for the peaks to be eroded away. If  $b > a$ , this stabilizing effect prevails over the destabilizing effect of the curvature dependence of the sputter yields, and the amplitude of the small- $k$  surface disturbance attenuates to zero.

In addition to explaining the formation of well-ordered hexagonal arrays of nanodots, our theory makes the intriguing prediction that normal-incidence bombardment will produce surface ripples for sufficiently large values of  $\xi$ . Experimental observation of this morphology would provide compelling evidence for the validity of our theory.

Our theory also shows that hysteretic switching between different kinds of order can occur. For example, suppose SRHO is observed at a temperature  $T_{\text{hex}}$ . For a sufficiently high temperature  $T_{\text{flat}} > T_{\text{hex}}$ , the smoothing effect of surface diffusion will be predominant, and the surface will be flat. Consider what happens if  $T = T_{\text{flat}}$  initially, and then  $T$  is slowly reduced.  $\xi$  is a complex function of  $T$  that depends on material parameters that have not yet been measured (e.g.,  $\nu$  and  $\eta$ ). For simplicity, assume that

$\xi(T_{\text{flat}}) < -1/20$  and  $0 < \xi(T_{\text{hex}}) < 1$  and that  $\xi$  is a decreasing function of  $T$ . The surface remains flat as  $T$  is reduced until  $\xi$  reaches zero, and then an array of nanodots with SRHO begins to emerge. As time passes, the correlation length and the amplitude  $\mathcal{A}$  of the nanodot array grow, and in the steady state,  $\mathcal{A}$  saturates. The concentration of the species with the lower sputter yield is reduced at the top of the dots and enhanced in the depressions. If  $T$  is now gradually increased,  $\mathcal{A}$  remains nonzero, until, when  $\xi$  is just below the value  $-1/20$ ,  $\mathcal{A}$  drops to zero and the surface becomes flat once more. Analogous hysteretic switching between hexagonal patterns and rolls occurs for  $1 \leq \xi \leq 4$ .

Our theory is readily extended to oblique-incidence ion bombardment of binary compounds with sample rotation [13]. Once again, we find that nanodot arrays with short-range hexagonal ordering are formed for certain values of the parameters. Thus, a theory akin to the one advanced in this Letter is able to account for the pattern formation observed when InP is subjected to oblique-incidence ion bombardment with concurrent rotation of the sample [5].

- 
- [1] For example, see B. Ziberi *et al.*, *J. Phys. Condens. Matter* **21**, 224003 (2009).
  - [2] For a review, see E. Chason and W.L. Chan, *Top. Appl. Phys.* **116**, 53 (2010).
  - [3] R.M. Bradley and J.M.E. Harper, *J. Vac. Sci. Technol. A* **6**, 2390 (1988).
  - [4] S. Facsko *et al.*, *Science* **285**, 1551 (1999).
  - [5] F. Frost, A. Schindler, and F. Bigl, *Phys. Rev. Lett.* **85**, 4116 (2000).
  - [6] M. Cross and H. Greenside, *Pattern Formation and Dynamics in Nonequilibrium Systems* (Cambridge University Press, Cambridge, England, 2009).
  - [7] R. Cuerno and A.-L. Barabási, *Phys. Rev. Lett.* **74**, 4746 (1995).
  - [8] M. Castro *et al.*, *Phys. Rev. Lett.* **94**, 016102 (2005).
  - [9] S. Facsko *et al.*, *Phys. Status Solidi B* **224**, 537 (2001).
  - [10] V.B. Shenoy, W.L. Chan, and E. Chason, *Phys. Rev. Lett.* **98**, 256101 (2007).
  - [11] G. Carter and V. Vishnyakov, *Phys. Rev. B* **54**, 17647 (1996); M. Moseler *et al.*, *Science* **309**, 1545 (2005); B. Davidovitch, M.J. Aziz, and M.P. Brenner, *Phys. Rev. B* **76**, 205420 (2007).
  - [12] S. Facsko *et al.*, *Phys. Rev. B* **69**, 153412 (2004).
  - [13] P.D. Shipman and R.M. Bradley (unpublished).
  - [14] O. Plantevin *et al.*, *Appl. Phys. Lett.* **91**, 113105 (2007).
  - [15] J. Muñoz-García *et al.*, *Phys. Rev. Lett.* **104**, 026101 (2010).
  - [16] J. Muñoz-García, R. Cuerno, and M. Castro, *J. Phys. Condens. Matter* **21**, 224020 (2009).
  - [17] P. Sigmund, *J. Mater. Sci.* **8**, 1545 (1973).
  - [18] M.A. Makeev, R. Cuerno, and A.-L. Barabási, *Nucl. Instrum. Methods Phys. Res., Sect. B* **197**, 185 (2002).
  - [19] V. Tuboltsev *et al.*, *Phys. Rev. B* **72**, 205434 (2005).
  - [20] M.Z. Hossain, J.B. Freund, and H.T. Johnson, *J. Appl. Phys.* **103**, 073508 (2008).